Communication: Distinguishing between short-time non-Fickian diffusion and long-time Fickian diffusion for a random walk on a crowded lattice

Adam J. Ellery,[1] Ruth E. Baker,[2] and Matthew J. Simpson[1]
[1]*School of Mathematical Sciences, Queensland University of Technology (QUT), Brisbane, Australia*
[2]*Mathematical Institute, University of Oxford, Radcliffe Observatory Quarter, Woodstock Road, Oxford, United Kingdom*

(Received 18 February 2016; accepted 26 April 2016; published online 5 May 2016)

The motion of cells and molecules through biological environments is often hindered by the presence of other cells and molecules. A common approach to modeling this kind of hindered transport is to examine the mean squared displacement (MSD) of a motile tracer particle in a lattice-based stochastic random walk in which some lattice sites are occupied by obstacles. Unfortunately, stochastic models can be computationally expensive to analyze because we must average over a large ensemble of identically prepared realizations to obtain meaningful results. To overcome this limitation we describe an exact method for analyzing a lattice-based model of the motion of an agent moving through a crowded environment. Using our approach we calculate the exact MSD of the motile agent. Our analysis confirms the existence of a transition period where, at first, the MSD does not follow a power law with time. However, after a sufficiently long period of time, the MSD increases in proportion to time. This latter phase corresponds to Fickian diffusion with a reduced diffusivity owing to the presence of the obstacles. Our main result is to provide a mathematically motivated, reproducible, and objective estimate of the amount of time required for the transport to become Fickian. Our new method to calculate this crossover time does not rely on stochastic simulations. *Published by AIP Publishing.* [http://dx.doi.org/10.1063/1.4948782]

I. INTRODUCTION

Modeling the transport of cells and molecules can be complicated because many biological environments are crowded with structures that can obstruct cellular and molecular motion. In the literature, this kind of hindered transport is often modeled using a lattice-based nearest neighbor random walk in which a proportion of lattice sites is populated with immobile obstacles.[1–11] In these simulations, crowding effects are modeled explicitly by enforcing an exclusion principle that prevents the motile agent from stepping onto any site that is occupied by obstacles.[12] Mean squared displacement (MSD) data from simulations indicate the existence of a transition period where, at first, the MSD does not follow a power law in time.[1,2,4,7–10] However, after a sufficiently long period of time, the MSD increases in proportion with time, and the transport process eventually becomes Fickian.[13–15] Since it is common to quantify biological transport in terms of a Fickian diffusivity, it is of interest to predict the amount of time required for the transport process to effectively reach the Fickian regime. We refer to this amount of time as the crossover time.

Here, we propose a new, exact method for calculating the transient MSD and crossover time for a lattice-based random walk in which the lattice is partially occupied by immobile obstacles. Our results do not depend on performing stochastic simulations. We apply existing results from Markov chain theory to show that the transient phase approaches the Fickian phase exponentially fast. Using this information we present an objective, mathematically based estimate of the crossover time using the concept of mean action time.[16–18]

II. STOCHASTIC SIMULATIONS

We consider a two-dimensional square lattice, of dimension $X \times Y$, with unit lattice spacing. Sites are indexed (i, j) so that each site has location $(x, y) = (i, j)$. The lattice is randomly populated with obstacles, with density ϕ. A motile agent is placed on an unoccupied site and allowed to undergo a discrete time nearest neighbor random walk[22] with time steps of unit duration. Periodic boundary conditions are enforced on all boundaries. Crowding effects are modeled explicitly by aborting all potential motility events that would lead to the motile agent stepping to a site that is occupied by an obstacle.[12]

As the simulation proceeds, we record the displacement of the agent, $r(t)$, and we use this information to calculate the MSD, $\langle r^2(t) \rangle$, where $\langle \cdot \rangle$ denotes an average over a large ensemble of identically prepared realizations in which the motile agent has the same starting position in each realization. Several earlier studies[1,2,4,7] suggest that $\langle r^2(t) \rangle$ may evolve as a power law, $\langle r^2(t) \rangle = 4Dt^\alpha$, where $0 < \alpha < 2$ is a constant that indicates the type of transport taking place.[15] Subdiffusion is associated with $\alpha < 1$, superdiffusion is associated with $\alpha > 1$, and classical Fickian diffusion is associated with $\alpha = 1$. To explore this power law behavior, we follow a standard approach by plotting $\log_{10}(\langle r^2(t) \rangle / t)$ as a function of $\log_{10}(t)$.[1,2] If the MSD follows this power law, the data in this plot should fall on a straight line. If the power law holds,

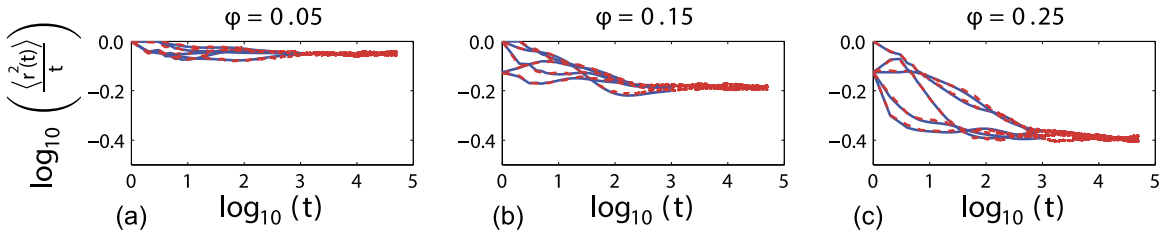

FIG. 1. (a)–(c) show $\log_{10}(\langle r^2(t)\rangle/t)$ as a function of $\log_{10}(t)$ for five randomly chosen starting positions on lattices with $\phi = 0.05$, 0.15, and 0.25, respectively. Exact results, calculated using the Markov chain approach (solid blue), are superimposed on results from stochastic simulations (dashed red). All results correspond to $X = Y = 10^3$, and simulation data are averaged over 10^4 identically prepared realizations. The exact solution is calculated until $t = 10^3$, whereas the stochastic simulations are calculated until $t = 5\times10^4$.

the straight line will have a negative slope if $\alpha < 1$, a positive slope if $\alpha > 1$, or it will be a horizontal line if the transport is Fickian and $\alpha = 1$.

Results in Figures 1(a)–1(c) show stochastic MSD data for $\phi = 0.05, 0.15$, and 0.25, respectively. In each subfigure we show plots of $\log_{10}(\langle r^2(t)\rangle/t)$ as a function of $\log_{10}(t)$ for five randomly chosen starting locations. After a sufficiently large amount of time, each MSD curve, for each value of ϕ, appears to approach to the same, approximately horizontal, straight line. This is consistent with previous analysis since the MSD is proportional to t, giving $\langle r^2(t)\rangle = 4Dt$, in the long time limit,[19,20] as $t \to \infty$. In this case, the crowded Fickian diffusivity, D, is reduced relative to the standard obstacle-free diffusivity, $D_0 = 1/4$ in two dimensions on a unit lattice, and the value of D depends on ϕ. For each value of ϕ considered in Figure 1, we observe a different horizontal asymptote, and we see that D decreases with ϕ.

All stochastic simulation results in Figure 1 are obtained by performing many identically prepared realizations of a random walk in which the initial location of the motile agent is held constant. Additional results, given in Figure 2, are obtained by performing many identically prepared realizations of a random walk in which the initial location of the motile agent is chosen randomly in each realization. Since the MSD data in Figures 2(a)–2(c) are further averaged over different starting locations, we denote the MSD data in Figure 2 as $\langle \bar{r}^2(t)\rangle$. For each value of ϕ, the MSD data in Figure 2 form a curve which, like the data in Figure 1, eventually asymptotes to a horizontal line after a sufficient amount of time.[1,2,4,7]

Now that we have presented standard MSD data from a stochastic random walk algorithm in Figures 1 and 2, we aim to present some analysis allowing us to predict key features of the simulated data without the need for performing stochastic simulations.

III. ANALYSIS

Let $\mathbf{p}(t)$ be a vector whose kth element denotes the probability of finding the motile agent at the kth lattice site at time t. The evolution of $\mathbf{p}(t)$ is given by the Markov chain

$$\mathbf{p}(t) = \mathbf{p}(0)\,\mathbf{T}^t, \tag{1}$$

where $\mathbf{T}$ is the transition matrix[21,22] and the superscript t indicates exponentiation to the value of time, t. The elements of $\mathbf{T}$, $T_{a,b}$, denote the probability that the agent will step from site a to site b per time step. Evaluating Equation (1) in a computationally efficient manner is challenging. Although $\mathbf{T}$ is sparse, $\mathbf{T}^t$ is not, and even a modestly sized lattice may require several petabytes to store and manipulate. To manage computational limitations, we evaluate Equation (1) iteratively at discrete time steps, $t_m = m$, for $m = 0,1,2,3,\ldots$. This allows us to take advantage of the relation $\mathbf{p}(t) = \left(\mathbf{p}(0)\mathbf{T}^{t-1}\right)\mathbf{T}$, from which it follows that

$$\mathbf{p}(t_m) = \mathbf{p}(t_{m-1})\,\mathbf{T}, \quad \forall\, m = 1,2,3,\ldots \tag{2}$$

This approach allows us to calculate $\mathbf{p}(t)$ by storing just $\mathbf{p}(t_m)$ and the sparse transition matrix, $\mathbf{T}$.

Simulation data in Figures 1 and 2 are obtained by imposing periodic boundary conditions. To evaluate the MSD in the simulations we record the number of times that the motile agent crosses the boundaries of the lattice to arrive at a particular site. However, in our analysis, the vector $\mathbf{p}(t)$ does not contain any information about the number of times that the agent crosses the lattice boundaries. To deal with this analytically, we consider a large lattice that is composed of a

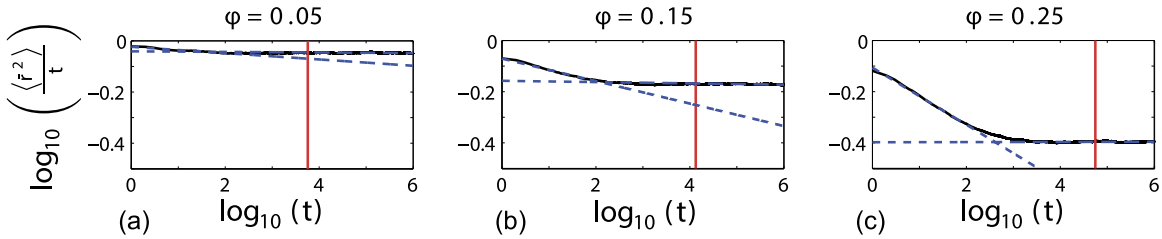

FIG. 2. (a)–(c) show plots of $\log_{10}(\langle \bar{r}^2(t)\rangle/t)$ as a function of $\log_{10}(t)$ for $\phi = 0.05$, 0.15, and 0.25, respectively (solid black). In each case the logarithm of the crossover time, $\log_{10}(C)$, is superimposed (vertical red). The least–squares best fit straight lines for *early* time data ($0 \le t \le 10^2$) and *late* time data ($10^4 \le t \le 10^6$) are also given (blue–dashed). The ordinate of the intersection of these fitted straight lines is Saxton's crossover time.[1,2] All simulations use $X = Y = 25$, and averaged MSD data are generated using 5×10^4 identically prepared realizations. The MSD data are generated until $t = 10^6$.

periodic tiling of the smaller lattice used in the simulations. The tiling is chosen to be sufficiently large to ensure that the probability that the agent reaches the boundaries of the larger tiled lattice during the time interval considered is zero. Because $\mathbf{p}(t)$ is the exact probability of locating the agent at any site at time t, we calculate the MSD exactly, without considering an ensemble

$$r^2(t) = \sum_{i,j} x^2_{i,j}(t)\, p_{ij}(t), \tag{3}$$

where $x^2_{i,j}(t) = [i(t) - i(0)]^2 + [j(t) - j(0)]^2$ and $p_{ij}(t)$ denotes the probability of finding the agent at site (i, j), on the tiled lattice, at time t. At each discrete value of time, we use Equation (3) to calculate the exact value of $r^2(t)$. We apply Equations (2) and (3) to mimic the stochastic simulation data in Figure 1. Exact results are superimposed on averaged simulation results in Figures 1(a)–1(c). For each of ϕ, and for each of the five starting positions we find that the Markov chain calculation compares very well with the averaged stochastic simulation data. Exact and simulation data in Figure 1 are compared for $t < 10^3$ since it becomes increasingly expensive to evaluate the exact results for larger t.

IV. CROSSOVER TIME

Transport of single cells or molecules is often quantified in terms of a Fickian diffusivity. Therefore, we are interested in predicting the amount of time required for the transport process to effectively reach the Fickian regime. Previous estimates of the crossover time have been obtained using simulation data. For example, Saxton[1,2] obtained averaged stochastic MSD data and fitted two straight lines to those data. The first straight line is fitted to the small time, early portion of the MSD data. The second straight line is fitted to the large time, late portion of the MSD data. Using this approach, Saxton estimated the crossover time by finding the time at which these two straight lines intersect. This method suffers from the limitation that it requires the generation of stochastic simulation data. Furthermore, the choice of fitting straight lines to *early* and *late* time data involves making subjective choices. In particular, without an objective definition of *early* time and *late* time, this definition of crossover time is not reproducible. In contrast, we provide a mathematically motivated and reproducible estimate of the crossover time that avoids performing stochastic simulations.

The rate at which $\mathbf{p}(0)\mathbf{T}^t$ approaches $\mathbf{p}(0)\mathbf{\Pi}$ is bounded by an exponential (Appendix A), with rate $\lambda_2^t = \mathrm{e}^{\log_e(\lambda_2)\, t}$, where λ_2 is the real eigenvalue of $\mathbf{T}$ that has the second-largest magnitude. Using this bound, together with the theory of mean action time (Appendix B), we provide a finite estimate of the crossover time,

$$C = -\frac{2}{\log_e \lambda_2}. \tag{4}$$

This definition of crossover time is simpler to implement than Saxton's[1,2] approach because we do not need to perform stochastic simulations, nor do we need to make subjective choices about fitting straight lines to *early* time and *late* time simulation data.

In practice, it is straightforward to calculate λ_2 using the following algorithm: (i) calculate the eigenvector, $\mathbf{u}$, corresponding to the leading eigenvalue of $\mathbf{T}$ using the power–iteration method,[23] (ii) calculate Hotelling's deflated matrix,[23] $\mathbf{A} = \mathbf{T} - \lambda_1 \mathbf{v}\mathbf{v}^{\mathrm{T}}$, where $\mathbf{v} = \mathbf{u}/|\mathbf{u}|$ and the superscript $^{\mathrm{T}}$ denotes a transpose, and (iii) apply the power–iteration method a second time to the matrix $\mathbf{A}$ and use the Rayleigh coefficient $\lambda_2 = \mathbf{w}^{\mathrm{T}}\mathbf{A}\mathbf{w}/\mathbf{w}^{\mathrm{T}}\mathbf{w}$, where $\mathbf{w}$ is the eigenvector of the leading eigenpair of $\mathbf{A}$, to recover λ_2.

Results in Figures 2(a)–2(c) show $\log_{10}(C)$ superimposed on the simulated MSD curves. Visually, the values of C appear to act as a useful estimate of the crossover time because the simulated MSD curves appear to be effectively horizontal for $t > C$. In particular, we have $C = 0.57 \times 10^4$, 1.3×10^4, and 5.6×10^4 for $\phi = 0.05$, 0.15, and 0.25, respectively. These results show that the crossover time increases with ϕ, as we might anticipate. In Figures 2(a)–2(c) we also show the least–squares best fit straight lines for both *early* and *late* time. The intersection of these straight lines gives Saxton's crossover time. In these cases we have $C_{\mathrm{Saxton}} = 0.37 \times 10^2$, 1.2×10^2, and 4.1×10^2 for $\phi = 0.05, 0.15$, and 0.25, respectively. These estimates are two orders of magnitude smaller than the estimates given by our new definition. We note that, unlike Saxton's method, our approach is based on an objective mathematical definition, is reproducible, and does not require any stochastic simulations.

V. DISCUSSION

We present an exact method for modeling the motion of a tracer particle on a crowded lattice. The Markov chain method leads to exact calculations of the probability of finding an agent at a site at any time, and from this information we can calculate the MSD exactly. These exact results compare very well with simulation data.

Our analysis shows that λ_2^t is an upper bound for the difference between a vector describing the time dependent probabilities of finding an agent at any site, and the long time limit. Here, λ_2 is the real eigenvalue of $\mathbf{T}$ that has the second–largest magnitude. Since we have exponential decay, we use the theory of mean action time to define an objective, mathematically motivated estimate of the amount of time required to effectively reach the long time limit. Therefore, our mathematically motivated definition of crossover time is less subjective than previous approaches that rely on generating stochastic data and fitting straight lines to those data.[1,2]

Our analysis of the crossover time is useful if we wish to implement the previous analysis of Mercier and Slater.[19,20] Mercier and Slater describe a method for calculating the long time Fickian diffusivity, D, for a lattice-based random walk in which a proportion of the sites is occupied by obstacles. An implicit assumption in applying Mercier and Slater's algorithm is that the transport process has been taking place for a sufficiently long period of time because this analysis is relevant only in the long time limit, $t \to \infty$. To implement Mercier and Slater's approach, one must first decide whether

a sufficient amount of time has passed so that the long time limit is relevant. Our approach for calculating C provides this information without performing simulations.

Although this manuscript focuses on two–dimensional examples, our definition of C, and the approach for calculating C, applies directly to three–dimensional lattices without any modification.

ACKNOWLEDGMENTS

This work is supported by the Australian Research Council (Grant Nos. DP140100249 and FT130100148). We thank two anonymous reviewers for their suggestions.

APPENDIX A: DERIVATION OF UPPER BOUND

We begin by considering the long time limit of $\mathbf{p}(t)$, $\lim_{t\to\infty}\mathbf{p}(t) = \lim_{t\to\infty}\mathbf{p}(t-1)\mathbf{T} = \mathbf{p}(0)\,\mathbf{\Pi}$, where $\mathbf{\Pi} = \lim_{t\to\infty}\mathbf{T}^t$. The spectral norm of any square matrix, $\mathbf{A}$, is given by[24]

$$\|\mathbf{A}\|_2 = \sqrt{\lambda_{\max}\left\{\mathbf{A}^{\mathrm{H}}\mathbf{A}\right\}}, \tag{A1}$$

where $\|\cdot\|_2$ denotes the spectral norm, the superscript $^{\mathrm{H}}$ denotes a Hermitian transpose, and $\lambda_{\max}\{\cdot\}$ denotes the largest eigenvalue. The spectral norm of the difference between $\mathbf{p}(t)$ and $\lim_{t\to\infty}\mathbf{p}(t)$ satisfies a triangle inequality

$$\begin{aligned}\|\mathbf{p}(0)\mathbf{T}^t - \mathbf{p}(0)\mathbf{\Pi}\|_2 &\le \|\mathbf{p}(0)\|_2\|\mathbf{T}^t - \mathbf{\Pi}\|_2,\\ &\le \|\mathbf{T}^t - \mathbf{\Pi}\|_2,\end{aligned} \tag{A2}$$

where we have used the fact that $\|\mathbf{p}(0)\|_2 \equiv 1$. The quantity $\|\mathbf{T}^t - \mathbf{\Pi}\|_2$ is an upper bound for the magnitude of the difference between $\mathbf{p}(t)$ and $\lim_{t\to\infty}\mathbf{p}(t)$ at any time t. To quantify this upper bound, we note that, because $\mathbf{T}$ is symmetric, it is always diagonalizable,[23] giving $\mathbf{\Pi} = \lim_{t\to\infty}\mathbf{T}^t = \lim_{t\to\infty}\mathbf{V}\mathbf{D}^t\mathbf{V}^{-1}$. Furthermore, because $\mathbf{T}$ is doubly stochastic, the eigenvalues of $\mathbf{T}$ are all real and satisfy $|\lambda_k| \le 1$, for $k = 1,2,3,\ldots$. We arrange these eigenvalues by magnitude so that $\lambda_1 > \lambda_2 > \lambda_3 > \cdots$, with $\lambda_1 = 1$. The long time limit is therefore given by $\mathbf{\Pi} = \mathbf{V}\mathbf{D}^\infty\mathbf{V}^{-1}$, where $\mathbf{D}^\infty = \lim_{t\to\infty}\mathbf{D}^t = \mathrm{diag}\{1,0,\ldots,0\}$. This allows us to write $\mathbf{T}^t - \mathbf{\Pi} = \mathbf{V}\left(\mathbf{D}^t - \mathbf{D}^\infty\right)\mathbf{V}^{-1} = \mathbf{V}\mathbf{D}_a\mathbf{V}^{-1}$, where $\mathbf{D}_a = \mathrm{diag}\{0,\lambda_2^t,\ldots,\lambda_{n-1}^t\}$. Since $\mathbf{T}$ is symmetric, its eigenvectors form an orthonormal basis for $\mathbb{R}^{n\times n}$, where n is the number of vacant lattice sites. This also means that $\mathbf{V}$ is unitary[23] and satisfies $\mathbf{V}^{\mathrm{H}} = \mathbf{V}^{-1}$. Using these properties we can write

$$\begin{aligned}\left(\mathbf{T}^t - \mathbf{\Pi}\right)^{\mathrm{H}}\left(\mathbf{T}^t - \mathbf{\Pi}\right) &= \mathbf{V}^{-\mathrm{H}}\mathbf{D}_a\mathbf{V}^{\mathrm{H}}\mathbf{V}\mathbf{D}_a\mathbf{V}^{-1},\\ &= \mathbf{V}\mathbf{D}_a^2\mathbf{V}^{-1}.\end{aligned} \tag{A3}$$

The largest eigenvalue of $\mathbf{V}\mathbf{D}_a^2\mathbf{V}^{-1}$ is given by the second diagonal element of the diagonal matrix, λ_2^{2t}. Combining Equations (A1)-(A3) gives $\|\mathbf{p}(0)\mathbf{T}^t - \mathbf{p}(0)\mathbf{\Pi}\|_2 \le \lambda_2^t$. For modest sized lattices λ_2 can be calculated using the power-iteration method.[23]

APPENDIX B: MEAN ACTION TIME

To demonstrate the theory of mean action time, we consider $\dot{z}(t) = -kz(t)$, with $k > 0$, which is a model of exponential decay. McNabb and Wake[16] define $F(t) = 1 - z(t)/z(0)$, which is a monotonically increasing function of t that satisfies $F(0) = 0$ and $\lim_{t\to\infty}F(t) = 1^-$. If we consider $F(t)$ to act like a cumulative distribution function, the associated probability density function is $f(t) = -\dot{z}/z(0)$. The mean of this distribution can be thought of as a measure of the amount of time required for $z(t)$ to effectively asymptote to the long time limit, $\lim_{t\to\infty}z(t) = 0$. The mean of $f(t)$, called the mean action time, is $M = -(1/z(0))\int_0^\infty t\dot{z}(t)\,\mathrm{d}t$. For the exponential decay model we obtain $M = 1/k$. We can use M as a measure of the amount of time we required for $z(t)$ to *effectively* reach the long time limit.

Higher moments can be used to quantify the width of the distribution[17,18] of $f(t)$. The variance of $f(t)$ is given by $V = -(1/z(0))\int_0^\infty t^2\dot{z}(t)\,\mathrm{d}t$. For the exponential decay model we have $V = 1/k^2$. A useful definition of the amount of time required for $z(t)$ to effectively asymptote to the long time limit, accounting for the mean and the width of the distribution, is $M + \sqrt{V}$. Previous analysis of exponentially decaying laboratory data confirms that this definition leads to very useful results that are simple to implement.[25,26] Therefore, a mathematically motivated finite estimate of the amount of time required for the decay process to effectively reach the long time limit is $C = M + \sqrt{V}$. Or, for the exponential decay model, $C = 2/k$.

[1]M. J. Saxton, Biophys. J. **66**, 394 (1994).
[2]M. J. Saxton, Biophys. J. **72**, 1744 (1997).
[3]D. V. Nicolau, Jr., J. F. Hancock, and K. Burrage, Biophys. J. **92**, 1975 (2007).
[4]A. Wedemeier, H. Merlitz, C.-X. Wu, and J. Langowski, J. Chem. Phys. **131**, 064905 (2009).
[5]D. Lepzelter and M. H. Zaman, Biophys. J. **99**, L106 (2010).
[6]D. Lepzelter and M. H. Zaman, J. Chem. Phys. **137**, 175102 (2012).
[7]E. Vilaseca, A. Isvoran, S. Madurga, I. Pastor, J. Garcés, and F. Mas, Phys. Chem. Chem. Phys. **13**, 7396 (2011).
[8]A. J. Ellery, M. J. Simpson, S. W. McCue, and R. E. Baker, J. Chem. Phys. **140**, 054108 (2014).
[9]A. J. Ellery, R. E. Baker, and M. J. Simpson, Phys. Biol. **12**, 066010 (2015).
[10]A. J. Ellery, R. E. Baker, S. W. McCue, and M. J. Simpson, Physica A **449**, 74 (2016).
[11]S. K. Ghosh, A. G. Cherstvy, D. S. Grebenkov, and R. Metzler, New J. Phys. **18**, 013027 (2016).
[12]T. M. Liggett, *Interacting Particle Systems* (Springer, 2005).
[13]B. D. Hughes, *Random Walks and Random Environments* (Oxford University Press, 1995).
[14]H. M. Taylor and S. Karlin, *An Introduction to Stochastic Modeling* (Academic Press, 1994).
[15]E. A. Codling, M. J. Plank, and S. Benhamou, J. R. Soc. Interface **5**, 813–834 (2008).
[16]A. McNabb and G. C. Wake, IMA J. Appl. Math. **47**, 193 (1991).
[17]A. J. Ellery, M. J. Simpson, S. W. McCue, and R. E. Baker, Phys. Rev. E **85**, 041135 (2012).
[18]A. J. Ellery, M. J. Simpson, S. W. McCue, and R. E. Baker, Phys. Rev. E **86**, 031136 (2012).
[19]J. F. Mercier and G. W. Slater, J. Chem. Phys. **110**, 6050 (1999).
[20]J. F. Mercier and G. W. Slater, J. Chem. Phys. **110**, 6057 (1999).
[21]J. S. Rosenthal, SIAM Rev. **37**, 387 (1995).
[22]R. Serfozo, *Basics of Applied Stochastic Processes* (Springer, 2012).
[23]G. H. Golub and C. F. Van Loan, *Matrix Computations* (John Hopkins University Press, 1996).
[24]I. S. Gradshteyn and I. M. Ryzhik, *Tables of Integrals, Series, and Products* (Academic Press, 2000).
[25]M. J. Simpson, F. Jazaei, and T. P. Clement, J. Hydrol. **501**, 241 (2013).
[26]F. Jazaei, M. J. Simpson, and T. P. Clement, J. Hydrol. **532**, 1 (2016).